

Simultaneous surface texture classification and illumination tilt angle prediction

X. Lladó[†], A. Oliver[†], M. Petrou[‡], J. Freixenet[†], and J. Martí[†]

[†] Computer Vision and Robotics Group - IliA. University of Girona

[‡] Centre for Vision, Speech and Signal Processing. University of Surrey
{*llado,aoliver,jordif,joanm*}@*eia.udg.es*; *m.petrou@eim.surrey.ac.uk*

Abstract

In this paper we investigate the effect of the illuminant tilt rotation over surface textures by analysing a set of image texture features extracted from the co-occurrence matrix. From the behaviour of each texture feature, a simple method able to predict the illuminant tilt angle of test images is developed. Moreover, the method is also used to perform a texture classification invariant to the illuminant tilt angle rotation. This study and experimental results over different real textures show that the illumination tilt angle can be accurately predicted, as part of the texture classification process.

1 Introduction

The 2-dimensional texture in the image, the image texture, is produced by variation in both surface reflectance and surface relief. While the reflectance properties are intrinsic to the surface, the surface relief produces a pattern of shadings that depends strongly on the direction of the illumination [2]. Thus, the image texture created by a 3D surface texture changes with the imaging geometry as illustrated in figure 1. Therefore, given different images of the same texture under different illumination directions, a simple method for image texture feature extraction, such as that based on the use of the co-occurrence matrix, provides different feature values.

These changes in the illumination can introduce errors in a texture classification system, if the illumination direction is altered between training and classification. Most of the classification approaches proposed in the literature do not take into account the effect of illumination on the imaged scene, thus tacitly assuming that the illumination direction is constant. Very few works have been published on this topic. Leung and Malik [5] developed a texture classification scheme that identifies 3D “textons” in the Columbia-Utrecht database for the purpose of illumination and viewpoint invariant classification. Recently, Chantler et al. [3] presented a formal theory which demonstrates that changes in the tilt angle of the illumination direction make texture features to follow super-elliptical trajectories in multi-dimensional feature spaces. Based on their work, Penirschke et al. [8] developed an illuminant rotation invariant classification scheme.

In other applications of Computer Vision a correct estimation of illumination can play an important role. For instance, light estimation is apparent in all applications



Figure 1: Three images of the same surface texture sample captured using different illuminant tilt angles.

which use photometric measurements which obviously depend on the illumination. Weber and Cipolla [9] focus their attention on reconstruction problems and estimation of light-source.

In this paper we investigate the effect of the illuminant tilt rotation over surface textures by analysing a set of texture features extracted from the gray-level co-occurrence matrix (GLCM). From the behaviour of each texture feature, we develop a simple method able to predict the illuminant tilt angle¹ of unknown test images. Moreover, we use this prediction method to perform the classification of textures under varying illuminant tilt angle.

The rest of this work is organised as follows. In section 2, we analyse the behaviour of texture features in the feature space. The method to predict the illuminant tilt angle is explained in section 3. In section 4, the performance of the method is evaluated in two experimental trials: illuminant tilt angle prediction and texture classification. Finally, the work ends with conclusions and further work.

2 Co-occurrence matrix behaviour

The co-occurrence matrix [4] is a well known method used to extract texture features. In this work the co-occurrence matrices are implemented in an anisotropic way. That is, we analyse 4 different directions: 0° , 45° , 90° , and 135° , computing for each one the contrast feature for a fixed distance 1. This feature is defined as:

$$Contrast = \sum_{i=0}^{N-1} \sum_{j=0}^{N-1} (i-j)^2 P_{\theta,d}(i,j) \quad (1)$$

where $P_{\theta,d}(i,j)$ represents the probability that the grey level j follows the grey level i at a distance d and angle θ , and N is the number of gray levels in the image.

A set of 15 different textures have been used throughout the experimental trials presented in this work. Figure 2 shows one image of each texture captured under a specific direction of illumination. Note that almost all of them are isotropic textures (see the first

¹We define our camera axis parallel to the z-axis. Therefore, the illuminant tilt is the angle the illuminant vector makes with the x-axis when it is projected onto the x, y plane, ie the image plane. The illuminant slant is the angle that the illuminant vector makes with the camera axis.



Figure 2: One image of each of the fifteen sample textures.

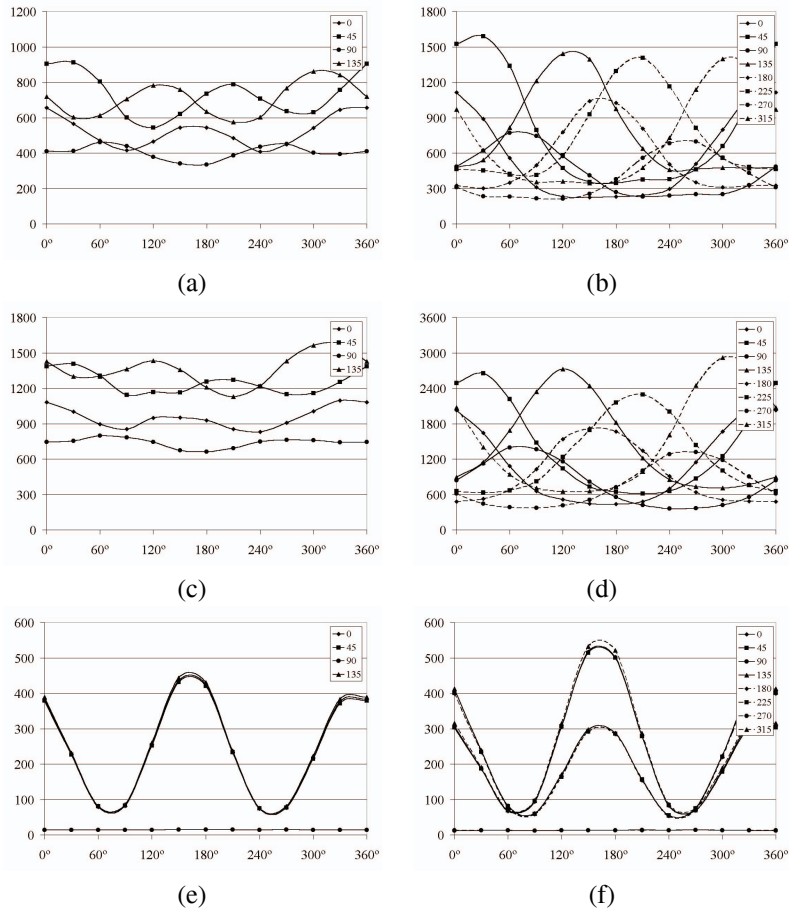


Figure 3: Feature behaviour for isotropic textures 1 (first row), and 9 (second row), and anisotropic texture 15 (third row). Each plot shows how one output of one feature (contrast at distance 1) varies when it is applied to the same physical texture sample, but under varying illuminant tilt angles (from 0° to 360°). (a), (c), and (e) Co-occurrence matrices computed for 4 different directions. (b), (d), and (f) Co-occurrence matrices computed for 8 different directions.

10 textures). Therefore, the only anisotropy in the image is induced by the anisotropic illumination. It is this anisotropy we wish to detect in order to identify the direction of illumination. We have included in the database some anisotropic textures as well for comparison. In order to detect anisotropy in an image we use the rotationally sensitive co-occurrence matrix from which we construct features.

Figures 3.(a), 3.(c) and 3.(e) illustrate the behaviour of these 4 features for textures 1, 9, and 15 respectively. Each plot shows how one output of one contrast feature varies when it is applied to the same texture sample, but under varying illuminant tilt angles (we use steps of 30° degrees from 0° to 360°).

Note that the graph of the anisotropic texture 15, which consists of long rough struc-

tures (see figure 2), shows some strange behaviour at first glance: three of the features behave in a very similar way (eg. note the three similar curves in figure 3.(e)) while one feature is totally constant. The catastrophic behaviour of this feature is due to the fact that the direction used to compute the corresponding co-occurrence matrix coincides with the direction of the long structures which make up the imaged surface. In this particular case, the images captured under all tilt angles have no significant intensity changes with respect to the axis of the local structures. Therefore, we obtain constant feature values for all tilt angles. On the other hand, when the long rough structures are illuminated from lateral directions, we expect some invariant behaviour as one side of these structures remains illuminated for a broad range of incident angles. This is the reason for which three of the features behave in a very similar way.

Moreover, observing the feature behaviour for isotropic textures we can see that the contrast feature at distance 1 has approximately a symmetric behaviour between ranges $[0^\circ, 180^\circ]$, and $[180^\circ, 360^\circ]$. Therefore, it is difficult to distinguish whether the illuminant tilt angle is in one or the other range. That is, by measuring one of these features, which is tilt angle sensitive, we may be able to identify the illuminant tilt angle only up to an ambiguity of $\pm 180^\circ$.

2.1 Removing the ambiguity from the estimation of the tilt angle

With the aim to improve the illuminant tilt angle prediction, allowing the estimation over the whole tilt rotation of 360° , we introduce the use of 4 new directions in the computation of the co-occurrence matrix. Therefore, we compute the co-occurrence matrix using 8 different directions: $0^\circ, 45^\circ, 90^\circ, 135^\circ, 180^\circ, 225^\circ, 270^\circ, 315^\circ$. Note that in this approach the co-occurrence matrix obtained for $180^\circ, 225^\circ, 270^\circ$, and 315° , are the transposed matrices of $0^\circ, 45^\circ, 90^\circ$, and 135° respectively. Hence, computing the classical contrast feature for these 8 matrices we only obtain 4 different values, since the contrast feature gives us the same value for a matrix and its transposed.

As our objective is to distinguish the sense of the directions used in the co-occurrence matrix, we propose to compute the contrast feature from the upper triangular matrix only. Therefore, equation 1 may be rewrite as:

$$Contrast = \sum_{i=0}^{N-1} \sum_{j=i}^{N-1} (i-j)^2 P_{\theta,d}(i,j) \quad (2)$$

We do that, with the idea to count the pairs of pixels in which the intensity value increases (transitions of darker pixels to brighter pixels). That can be seen from figures 3.(b) and 3.(d) where we plot the variation of these 8 new features for the isotropic textures 1 and 9. Note that for each tilt angle, the maximum value of the contrast feature is attained by the feature which has been computed from the co-occurrence matrix with the same orientation angle as the tilt angle. This is because we always find more transitions of darker pixels to brighter pixels when the orientation of the light source “coincides” with the orientation of the co-occurrence matrix. It is important to clarify that we use the term “coincide” when we refer to the same angle, but under two reference systems: one which defines the direction used in the co-occurrence matrix, and one which defines the direction of the incident light.

In contrast, the anisotropic textures do not follow this behavior (see figure 3.(f)), although they still exhibit an approximately symmetric behaviour over the two ranges of

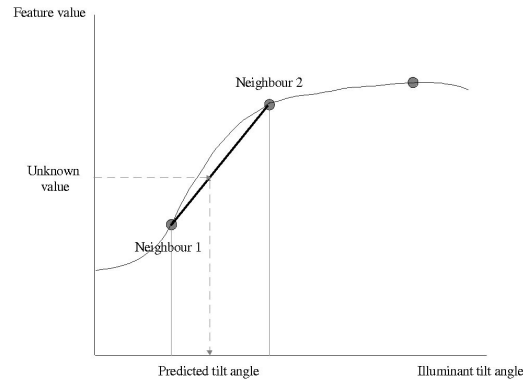


Figure 4: Prediction scheme. In a first step we find the two feature vectors (neighbour 1 and 2) closest to the analysed feature vector. Then, the tilt angle is obtained in the current interval applying a linear interpolation individually for each single feature.

values, namely $[0^\circ, 180^\circ]$, and $[180^\circ, 360^\circ]$.

The feature behaviour described in this section will be used as a model in order to predict the tilt angle of an unknown texture image. Each texture model is created using a small number of different tilt angles. Specifically, we have used 12 tilt angles 30° apart. Hence, a texture model is composed of 12 vectors of 8 features each (12 tilt angles, 8 directional co-occurrence matrices for each one of them).

3 Illuminant tilt angle prediction

The process of predicting the illuminant tilt angle given an unknown test image, starts by extracting a representative feature vector for this image, which implies the computation of 8 texture features. Note that the model of each texture is composed of 12 different feature vectors, one for each reference tilt angle.

When the feature vector for the unknown image is obtained, the prediction consists in looking for the most similar feature vector among the model textures. Then, a simple method of three steps is proposed:

- First, we obtain a first approximation of the predicted angle with one of the known angles used to describe the model texture. The nearest neighbour classifier is used to find the closest feature vector.
- After that, we localise the angle interval which contains the test feature vector. We use again the nearest neighbour classifier to find the second most similar feature vector of the same model texture (see figure 4). In this second step we ensure that the angle interval is of 30° . That means that the second known angle is $\pm 30^\circ$ with respect to the first approximation.
- Next, the exact tilt angle is found in the current interval applying linear interpolation for each single feature. The results are averaged to produce the final predicted

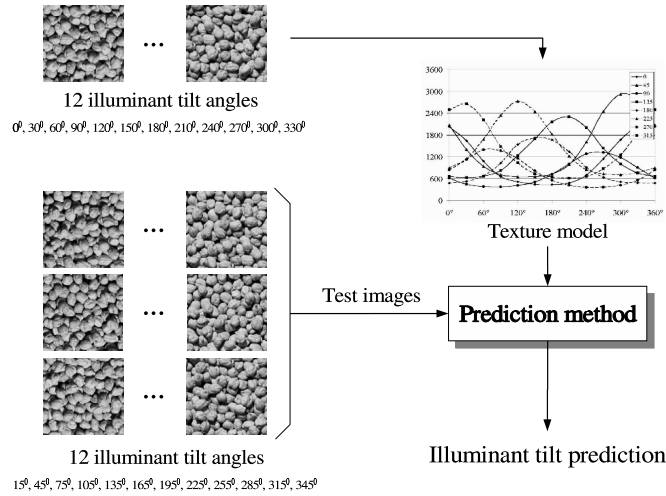


Figure 5: Experimental setup. Four different surface patches are available for each texture. One is used for modelling the feature behaviour, and the remaining ones are used for testing.

tilt angle. The tilt angles computed from individual features for which the linear interpolation provides slopes close to zero are not considered in the averaging process.

4 Experimental trials

The proposed prediction method was tested with 15 different textures. The first 10 were isotropic textures and the remaining five were anisotropic. For each one, 4 complete sets of 24 images corresponding to the illuminant tilt angles between 0° and 360° incremented in steps of 15° are available. All these images are illuminated at a slant angle of 55° . From these images we create 2 different sets: one used for modeling the illuminant behaviour, and another one used for testing the classification process.

The first set is composed of $15 \text{ textures} \times 12 \text{ illumination directions} = 180$ images. The 12 illuminant tilt angles used for modeling are $0^\circ, 30^\circ, 60^\circ, 90^\circ, 120^\circ, 150^\circ, 180^\circ, 210^\circ, 240^\circ, 270^\circ, 300^\circ,$ and 330° . On the other hand, the testing set is composed of $15 \text{ textures} \times 12 \text{ illumination directions} \times 3 \text{ images} = 540$ test images. The 12 illuminant tilt angles used for testing are different from the reference tilt angles mentioned above. Figure 5 illustrates the configuration used in our experimental trials.

4.1 Accuracy of tilt angle prediction

This experiment has as purpose to evaluate the accuracy of the illuminant tilt angle prediction. After computing the model behaviour, we apply individually for each texture the prediction method for all the corresponding test images.

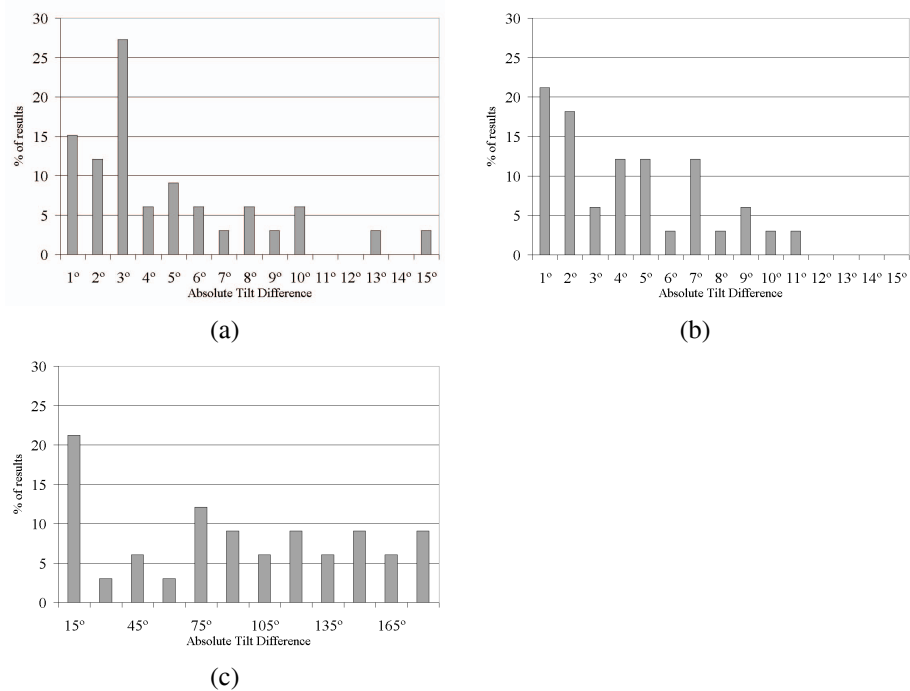


Figure 6: Error in the tilt angle prediction for textures 1, 9, and 15, (a), (b), and (c) respectively.

Figure 6 shows the error distributions for textures 1, 9, and 15 of the absolute tilt angle difference between our predictions and the correct values. Each plot has been computed for the 36 test images available for each texture and shows the percentage of times a particular error value was observed. Note that for isotropic textures 1 and 9, we predict the tilt angle for almost all the test images with an error of a few degrees. However, for texture 15 the errors are significantly larger.

From the error distributions of all 15 textures we conclude that for isotropic textures the illuminant tilt angle may be predicted quite accurately. However, poor results are obtained for anisotropic textures. We confirm this conclusion providing an overall quantitative assessment over all these predictions (see table 1). We have computed over all textures the average *MSE* of the tilt angle prediction and its standard deviation. In the same table we also present a quantitative assessment for the isotropic and anisotropic textures separately. It is important to remark that we predict the tilt angle for isotropic textures with an average error of 6° . Nevertheless, the prediction error is increased when anisotropic textures are considered. This is because the anisotropy of the image cannot be solely attributed to the illumination direction and therefore the detected anisotropy does not give us the clear and unambiguous information which is needed by our prediction method.

| Isotropic | | Anisotropic | | Overall | |
|-----------|------|-------------|-------|---------|-------|
| Avg | Std | Avg | Std | Avg | Std |
| 5.96 | 1.85 | 59.61 | 22.57 | 23.84 | 28.86 |

Table 1: Overall quantitative assessment over all 15 textures of illuminant tilt angle predictions. Average MSE and its standard deviation for the tilt angle difference between the predicted and true values.

4.2 Accuracy of texture classification

This experiment analyses the accuracy of the texture classification when our feature behaviour models are used as references for classification.

The method described in section 3 may be used not only to predict the illuminant tilt angle of a test image, but also to classify the unknown test image into one of the texture classes present in the database. Specifically, the first step in which the nearest neighbour classifier is used to find the closest feature vector to the model, allows us also to perform texture classification.

Table 2 summarises the obtained texture classification results when all fifteen models are used in the classification process. The texture classification accuracy is 82.63%, while the illuminant tilt angle is predicted with an average MSE of 24.04° and standard deviation of 43.07° . We have repeated the same experiment but using only the isotropic textures, achieving a texture classification accuracy of 79.09%. In this case, the illuminant tilt angle is predicted with an average MSE of 5.88° and standard deviation of 4.80° . Note that when using all fifteen textures we obtain better classification results than those using only isotropic textures. That is because isotropic textures have similar feature behaviour. For instance, test images of textures 2 and 4 have been misclassified. In contrast, as is shown in figure 3.(f), anisotropic textures have different feature behaviour. This fact causes the improvement of the classification rate, when anisotropic textures are included in the reported results. However, it is important to notice that accurate tilt angle predictions are only obtained for isotropic textures.

5 Conclusions

We presented a simple method able to predict the illuminant tilt angle of unknown test images. The method is based on behaviour models of texture features extracted from the co-occurrence matrix. It works under the assumption that the only anisotropy in the image is induced by the anisotropic illumination. The experimental results over different real textures, including some anisotropic textures for comparison, show that the illumination tilt angle can be accurately predicted. As well as predicting the illuminant tilt angle, the method is used to perform texture classification. The results show that anisotropic textures may be classified more accurately, but their illuminat tilt angle may not be predicted well, while isotropic textures cause more confusion to the classifier, but allow one to predict the direction from which the imaged surfaces were illuminated very accurately, as long as reference images for 12 different tilt angles of each surface are available. Such reference images may be created either by direct image capture when creating the ref-

| | Texture classification | Tilt angle MSE | |
|--------------------|------------------------|----------------|-------|
| | | Avg | Std |
| Isotropic textures | 79.09% | 5.85 | 4.80 |
| All textures | 82.63% | 24.06 | 43.07 |

Table 2: Texture classification rates and MSE of the tilt angle prediction obtained over the isotropic textures, and over all fifteen textures.

erence database, or from surface and colour information recovered by 4 source colour photometric stereo [1] and subsequent image rendering [6, 7].

Acknowledgment

This work was supported by UdG grant BR00/03, and by EPSRC grant GR/M73361.

References

- [1] S. Barsky and M. Petrou. The 4-source photometric stereo technique for 3-dimensional surfaces in the presence of highlights and shadows. *IEEE Transactions on Pattern Analysis and Machine Intelligence*, to appear, 2003.
- [2] M.J. Chantler. Why illuminant direction is fundamental to texture analysis. *IEE Proceedings in Vision, Image and Signal Processing*, 142(4):199–206, August 1995.
- [3] M.J. Chantler, M. Schmidt, M. Petrou, and G. McGunnigle. The effect of illuminant rotation on texture filters: Lissajous’s ellipses. In *7th European Conference on Computer Vision*, volume 3, pages 289–304, Copenhagen, Denmark, May 2002.
- [4] R.M. Haralick, K.S. Shanmugan, and I. Dunstein. Textural features for image classification. *IEEE Transactions on Systems, Man, and Cybernetics*, 3(6):610–621, 1973.
- [5] T. Leung and J. Malik. Representing and recognising the visual appearance of materials using three-dimensional textons. *International Journal of Computer Vision*, 43(1):29–44, June 2001.
- [6] X. Lladó, J. Martí, and M. Petrou. Classification of textures seen from different distances and under varying illumination direction. In *IEEE International Conference on Image Processing*, to appear 2003.
- [7] X. Lladó, M. Petrou, and J. Martí. Texture recognition under varying imaging geometries. *IEEE Transactions on Image Processing*, in second revision, 2003.
- [8] A. Penirschke, M.J. Chantler, and M. Petrou. Illuminant rotation invariant classification of 3d surface textures using lissajous’s ellipses. In *2nd international workshop on texture analysis and synthesis*, pages 103–107, Copenhagen, Denmark, June 2002.
- [9] M. Weber and R. Cipolla. A practical method for estimation of point light-sources. In *British Machine Vision Conference*, pages 471–480, Manchester, September 2001.